ELSEVIER

Available online at www.sciencedirect.com

ScienceDirect

Journal of Solid State Chemistry 180 (2007) 1832–1839

JOURNAL OF
SOLID STATE
CHEMISTRY

www.elsevier.com/locate/jssc

A neutron diffraction study of the d^0 and d^{10} lithium garnets $Li_3Nd_3W_2O_{12}$ and $Li_5La_3Sb_2O_{12}$

Edmund J. Cussen*, Thomas W.S. Yip

WestCHEM, Department of Pure and Applied Chemistry, Thomas Graham Building, University of Strathclyde, 295 Cathedral Street,
Glasgow G1 1XL, Scotland

Received 16 January 2007; received in revised form 5 April 2007; accepted 5 April 2007

Abstract

The garnets $Li_3Nd_3W_2O_{12}$ and $Li_5La_3Sb_2O_{12}$ have been prepared by heating the component oxides and hydroxides in air at temperatures up to 950 °C. Neutron powder diffraction has been used to examine the lithium distribution in these phases. Both compounds crystallise in the space group $Ia\bar{3}d$ with lattice parameters $a = 12.46869(9)$ Å ($Li_3Nd_3W_2O_{12}$) and $a = 12.8518(3)$ Å ($Li_5La_3Sb_2O_{12}$). $Li_3Nd_3W_2O_{12}$ contains lithium on a filled, tetrahedrally coordinated 24*d* site that is occupied in the conventional garnet structure. $Li_5La_3Sb_2O_{12}$ contains partial occupation of lithium over two crystallographic sites. The conventional tetrahedrally coordinated 24*d* site is 79.3(8)% occupied. The remaining lithium is found in oxide octahedra which are linked via a shared face to the tetrahedron. This lithium shows positional disorder and is split over two positions within the octahedron and occupies 43.6(4)% of the octahedra. Comparison of these compounds with related d^0 and d^{10} phases shows that replacement of a d^0 cation with d^{10} cation of the same charge leads to an increase in the lattice parameter due to polarisation effects.

Keywords: Metal oxides; Garnets; Lithium conductors; Neutron diffraction

1. Introduction

Lithium garnets have been known for nearly four decades [2], but in the last few years these materials have become of renewed interest due to the high Li^+ conductivity reported in some garnets of unusual stoichiometry [3–5]. These garnets have been shown to be insensitive to air and moisture and are unreactive towards metallic lithium [4]. These attributes make them attractive candidates for operation as an electrolyte in an all solid-state secondary lithium battery.

The conventional garnet stoichiometry contains a mixture of cations on filled square antiprismatic, octahedral and tetrahedral sites in a 3:2:3 ratio to give a stoichiometry such as $Ca_3Al_2Si_3O_{12}$. The structure of this phase is shown in Fig. 1 [1]. The garnets $Li_3Ln_3Te_2O_{12}$ follow this stoichiometry and contain lithium on the tetrahedral site of the structure but show minimal ionic mobility with $\sigma_{600\,^\circ C} \approx 10^{-5}\,S\,cm^{-1}$ [6]. However, a number of lithium-containing garnets have long been known to form with unusual stoichiometries $Li_5Ln_3M_2O_{12}$ where M is a pentavalent cation such as Ta^{5+}, [7,8] Nb^{5+} or Sb^{5+} [9,10]. The Li^+ conductivity of $Li_5La_3Ta_2O_{12}$ and $Li_5La_3Nb_2O_{12}$ is around three orders of magnitude greater [3] than $Li_3Nd_3Te_2O_{12}$ and at room temperature, $\sigma_{RT} \approx 10^{-5}$, is comparable to other crystalline Li^+ electrolytes [11]. This dramatic change in properties is associated with a distribution of lithium across multiple coordination sites. Whereas $Li_3Nd_3Te_2O_{12}$ accommodates lithium in a filled tetrahedral site, the fast-ion conducting phases $Li_5La_3M_2O_{12}$ contain ca. 20% vacancies on this site with the remaining lithium occupying a distorted octahedron with considerable positional disorder [12]. In the series $Li_{5+x}Ba_xLa_{3-x}Ta_2O_{12}$, the positional disorder increases smoothly as a function of lithium content [13] suggesting that this displacement occurs to minimise the repulsion associated with the short Li–Li contacts that exist between

---

*Corresponding author. Fax: +44 141 548 4822.
E-mail address: Edmund.Cussen@Strath.ac.uk (E.J. Cussen).

0022-4596/$ - see front matter © 2007 Elsevier Inc. All rights reserved.
doi:10.1016/j.jssc.2007.04.007

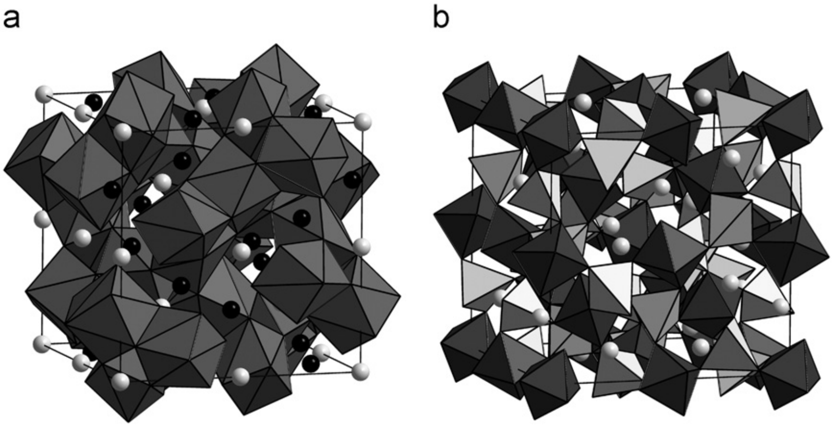

Fig. 1. The structure of a garnet such as $Ca_3Al_2Si_3O_{12}$ can be considered (a) to be based on a body-centred network of CaO_8 units containing aluminium (grey spheres) and silicon (black spheres) on the interstitial sites. An alternative representation (b) shows the continuous framework of corner sharing of AlO_6 (octahedra) and LiO_4 (tetrahedra) units with calcium occupying eight-coordinate interstitial sites.

the face-sharing tetrahedra and octahedra of oxide anions.

The structures of lithium-containing garnets have not been widely studied. Whilst structurally distorted garnets with reduced symmetry are known [14], the vast majority of garnets crystallise in the space group $Ia\bar{3}d$. The limited number of structural reports of lithium-containing garnets often describe these phases in lower symmetry cubic groups such as $I2_13$ [7,9,10,15] or $Ia\bar{3}$ [15] based on X-ray diffraction experiments which have poor sensitivity to lithium cations in these compounds. Here we present a neutron diffraction determination of the structure of two garnets $Li_3Nd_3W_2O_{12}$ and $Li_5La_3Sb_2O_{12}$. The structure of the former has not been reported and, as the only lithium garnets with a 3:3:2 stoichiometry that have been characterised are $Li_3Ln_3Te_2O_{12}$, this structural determination will show whether the observations in the tellurates are specific to that composition or applicable to lithium garnets in general. The structure of $Li_5La_3Sb_2O_{12}$ has been described in the space group $I2_13$ with lithium exclusively occupying a distorted octahedral position that is vacant in the usual garnet stoichiometry. We have recently found that the previous assignment of these structural features to both $Li_5La_3Ta_2O_{12}$ and $Li_5La_3Nb_2O_{12}$ was erroneous and thus the structure of $Li_5La_3Sb_2O_{12}$ merits reinvestigation. Both $Li_3Nd_3W_2O_{12}$ and $Li_5La_3Sb_2O_{12}$ also offer the chance to compare the similarities and differences between garnets containing d^0 and d^{10} cations and the impact of this on the structure.

2. Experimental

Initial attempts at synthesising both compounds using stoichiometric quantities of Nd_2O_3, WO_3, Sb_2O_3 and Li_2CO_3 ($Li_3Nd_3W_2O_{12}$) or $LiOH \cdot H_2O$ ($Li_5Nd_3Sb_2O_{12}$) consistently failed to produce single phase samples suitable for structural determination. The origin of this problem lies in the volatility of lithium oxide and in both cases it was necessary to use an excess of lithium in order to yield garnet phases. $Li_3Nd_3W_2O_{12}$ was prepared using a 5% stoichiometric excess of Li_2CO_3 and stoichiometric amounts of Nd_2O_3 and WO_3. These reagents were intimately ground in an agate mortar and pestle and pressed into pellets of 13 mm diameter. This pellet was then covered with powder of the same stoichiometry and heated in a covered alumina crucible from 650 to 750 °C at 0.5 °C min^{-1} and held at 750 °C for 2 days. The mixture was reground and repelleted several times and heated at 880 °C for a total of 5 days to give a product that X-ray powder diffraction measurements identified as a single phase. At no point was additional Li_2CO_3 added to the reaction mixture.

The preparation of $Li_5La_3Sb_2O_{12}$ was more complex. The synthesis of $Li_5La_3Sb_2O_{12}$ proceeded from a mixture of stoichiometric quantities of La_2O_3, Sb_2O_3 and $LiOH \cdot H_2O$. This mixture was pelleted and heated in an open alumina crucible for 24 h periods at temperatures up to 950 °C. Initial reactions produced a mixture of garnet, the perovskite La_2LiSbO_6 [16] and an unidentified minor impurity phase. Further heating of the mixture tended to increase the intensity of the Bragg peaks associated with the perovskite impurity whilst the introduction of additional $LiOH \cdot H_2O$ increased the intensity of the garnet peaks. Therefore, the addition of $LiOH \cdot H_2O$ was used to inhibit the formation of perovskite: when the quantity of perovskite was observed to be increasing, additional lithium hydroxide monohydrate was introduced into the mixture and the sample was heated from room temperature to 900 °C at 2.5 °C min^{-1}. The complete details of the heating regime are provided as Supplementary information.

The progress of reactions was followed using a Philips Xpert powder diffractometer operating with Cu$K\alpha$ radiation in Bragg Brentano geometry. Data were collected from the final products mounted on an aluminium slide over the range $10 \leqslant 2\theta \leqslant 80$ using a step size of $\Delta 2\theta = 0.02°$. Neutron diffraction data were collected using the time-of-flight diffractometer Polaris at Rutherford-Appleton Laboratory, Didcot, UK from ca. 2 g of sample contained in a cylindrical vanadium sample holder. This instrument uses three banks of detectors to collect data in the range $0.4 \leqslant d$ (Å) $\leqslant 8$. These data were analysed by Rietveld refinement [17] as implemented in the GSAS suite of programs [18] against data collected from all three data sets simultaneously. The peak shape was described by a convolution of pseudo-Voigt and double exponential functions, the latter

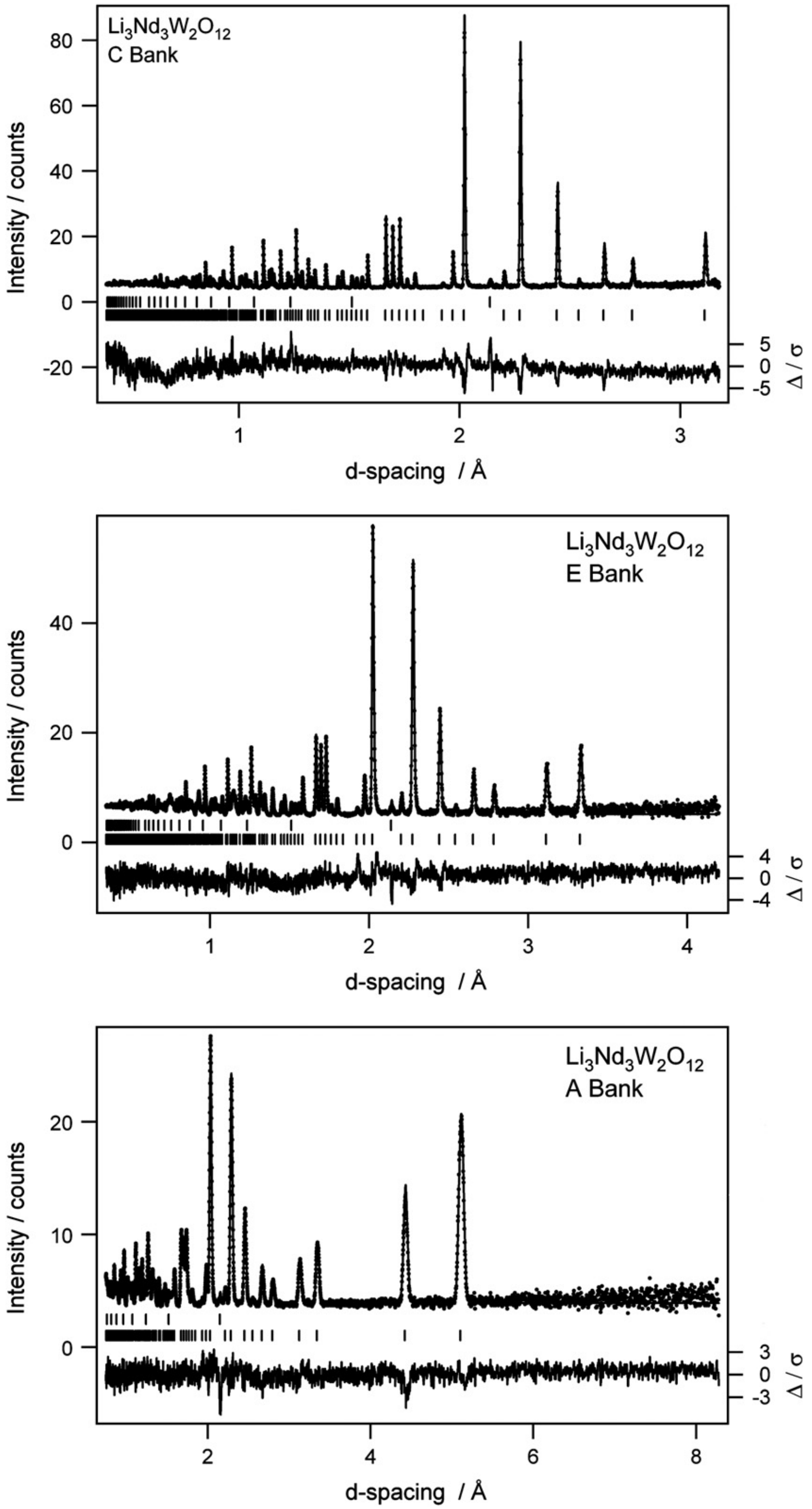

Fig. 2. Observed (dots) and calculated (line) neutron diffraction patterns collected from $Li_3Nd_3W_2O_{12}$ using the three banks of detectors of Polaris. The difference is presented as (I_{obs}–I_{calc})/[estimated standard deviation of I_{obs}] using the scale on the right axis. The upper and lower tick marks indicate Bragg reflections arising from the sample holder and the sample, respectively.

describing the contribution to the profile of the incident neutron pulse (Fig. 2).

3. Results

Previous reports of $Li_3Nd_3W_2O_{12}$ and $Li_5La_3Sb_2O_{12}$ have indicated that both of these compounds adopt the garnet structure. In the case of $Li_3Nd_3W_2O_{12}$ only lattice parameters were reported [2] and the structure of $Li_5La_3Sb_2O_{12}$ has been examined using X-ray diffraction [10], which is not anticipated to provide a precise description of the lithium distribution in this complex stoichiometry. Preliminary analysis of the X-ray diffraction data proceeded by comparison with diffraction data collected using the same instrument from two compounds with comparable compositions; namely $Li_3Nd_3Te_2O_{12}$ and $Li_5La_3Ta_2O_{12}$ [12]. Both of these compounds have been studied by neutron diffraction and have been found to crystallise in the space group, $Ia\bar{3}d$. X-ray diffraction data sets collected from both $Li_3Nd_3W_2O_{12}$ and $Li_5La_3Sb_2O_{12}$ could be completely indexed with the unique set of systematic absences associated with this space group using lattice parameters of 12.469 and 12.853 Å, respectively. In both cases the X-ray powder diffraction data could be modelled with a high level of accuracy using the non-lithium atoms on the conventional atomic positions for the garnet structure. The fit obtained against the data collected from $Li_5La_3Sb_2O_{12}$ is shown in Fig. 3.

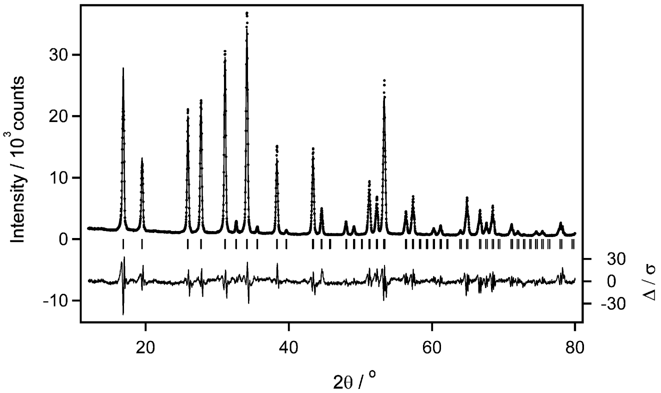

Fig. 3. Observed (dots) and calculated (line) X-ray powder diffraction patterns collected from $Li_5La_3Sb_2O_{12}$. The difference is presented as (I_{obs}–I_{calc})/[estimated standard deviation of I_{obs}] using the scale on the right axis.

Neutron diffraction data were collected from these compounds at room temperature in order to determine the lithium distribution. Data collected from $Li_3Nd_3W_2O_{12}$ contained Bragg peaks that could be fully indexed in the same space group as the X-ray diffraction data with the addition of a second phase to describe weak Bragg peaks arising from the vanadium sample container. These data were analysed using the structure of $Li_3Nd_3Te_2O_{12}$ as a starting model which readily refined to convergence. Alternative models which allowed occupancy of the octahedrally coordinated lithium position resulted in a refined fractional occupancy of this site of 0.001(4) indicating the complete absence of lithium on this position. Fixing the occupation of this site at a non-zero value of 0.1 and a reduction in occupation of the tetrahedral site to 0.8 in order maintain the correct stoichiometry lead to a clear degradation in the quality of fit with parameters $R_{wp} = 2.12$, $\chi^2 = 1.939$. The occupation of the octahedral position was set at zero and the occupancy of the tetrahedral site was fixed at unity and the refinement proceeded to convergence giving the fit parameters $R_{wp} = 2.00$, $\chi^2 = 1.715$ and the fit shown in Fig. 3. The atomic positions and displacement parameters from this refinement are collected in Tables 1 and 2, respectively. Selected interatomic distances are listed in Table 3.

A previous structural report of $Li_5La_3Sb_2O_{12}$ employed the space group $I2_13$ to fit X-ray diffraction data [10]. Whilst the X-ray powder diffraction data shown in Fig. 2 showed systematic absences that are uniquely associated with $Ia\bar{3}d$, the neutron diffraction data contained several other peaks which could not be indexed in a primitive cubic cell of the same dimensions as the garnet, suggesting that these are due to other phases. After a search of likely impurity phases it was found that the most intense of these

Table 1
Fit and structural parameters for $Li_3Nd_3W_2O_{12}$ and $Li_5La_3Sb_2O_{12}$ derived from refinement against neutron diffraction data

	R_{wp}	R_p	χ^2	a (Å)	Li 24d frac	Li 96h frac	Li(96h) x	Li(96h) y	Li(96h) z	O(96h) x	O(96h) y	O(96h) z
$Li_3Nd_3W_2O_{12}$	2.00	5.36	1.717	12.46869(9)	1	0	—	—	—	0.27863(2)	0.10750(20	0.19848(2)
$Li_5La_3Sb_2O_{12}$	1.69	2.29	2.181	12.8518(3)	0.793(8)	0.218(2)	0.1070(10)	0.6676(8)	0.6171(8)	0.27994(4)	0.10666(5)	0.19932(5)

Nd/La on 24c ($\frac{1}{8}$, 0, $\frac{1}{4}$), W/Sb on 16a (0, 0,0) , Li on 24d ($\frac{1}{4}$, $\frac{7}{8}$, 0), Li on 96h (x, y, z) and O on 96h (x, y, z).

Table 2
Displacement parameters for $Li_3Nd_3W_2O_{12}$ and $Li_5La_3Sb_2O_{12}$ derived from fitting neutron diffraction data

100U (Å^2)	Ln U_{11}	Ln $U_{22,\ 33}$	Ln U_{23}	Ln U_{eq}	M $U_{11,22,33}$	M $U_{12,13,23}$	M U_{eq}	Li U_{iso}	O U_{11}	O U_{22}	O U_{33}	O U_{12}	O U_{13}	O U_{23}	O U_{eq}
$Li_3Nd_3W_2O_{12}$	0.28(2)	0.185(8)	0.14(1)	0.22	0.241(9)	−0.055(12)	0.24	0.52(2)	0.465(10)	0.251(9)	0.546(11)	0.077(7)	0.030(8)	−0.077(8)	0.42
$Li_5La_3Sb_2O_{12}$	0.66(5)	1.25(3)	1.14(4)	1.05	0.43(2)	0.25(3)	0.43	2.00(10)	1.34(3)	0.50(3)	1.19(4)	–0.03(2)	–0.10(2)	–0.15(3)	1.01

Table 3
Selected interatomic distances (Å) and angles (deg) for $Li_3Nd_3W_2O_{12}$ and $Li_5La_3Sb_2O_{12}$

	$Li_3Nd_3W_2O_{12}$	$Li_5La_3Sb_2O_{12}$		$Li_5La_3Sb_2O_{12}$
Nd/La–O (×4)	2.4247(3)	2.5037(6)	Li(96*h*)–Li(Td)	1.738(9)
Nd/La–O (×4)	2.5097(3)	2.6011(7)	Li(96*h*)–Li(Td)	2.437(11)
⟨Nd/La⟩–O	2.4672	2.5524	Li(96*h*)–O	1.385(10)
O–Nd/La–O	101.358(10)	100.84(2)	Li(96*h*)–O	2.019(9)
			Li(96*h*)–O	2.582(14)
W/Sb–O (×6)	1.9229(3)	1.9914(6)	Li(96*h*)–O	2.336(13)
O–W/Sb–O	85.690(12)	86.52(3)	Li(96*h*)–O	2.771(9)
Li(Td)–O (×4)	1.9113(3)	1.9483(6)	Li(96*h*)–O	3.183(11)

peaks are due to Li_2CO_3, presumably formed by the dehydration of $LiOH \cdot H_2O$ to Li_2O during heating and then subsequent post-synthetic reaction of lithium oxide with atmospheric carbon dioxide. Weak Bragg peaks due to the vanadium sample container were also observed.

A Rietveld refinement [17] against these neutron diffraction data incorporated both of these minor phases and used the space group $Ia\bar{3}d$ and, based on observations in the related phases $Li_5La_3Nb_2O_{12}$ and $Li_5La_3Ta_2O_{12}$ [12], a mixture of tetrahedrally and octahedrally coordinated lithium to describe the garnet structure. The tetrahedral position (24*d*) has no positional variables and the lithium cation near the centre of the irregularly shaped octahedron (48 g) is constrained to $(\frac{1}{8}, y, \bar{y}+\frac{1}{4})$. The lithium distribution across these two crystallographic sites was allowed to vary with the constraint of maintaining five lithium cations per formula unit. Using an isotropic description of the lithium failed to give a satisfactory match to the observed data ($R_{wp} = 1.87$, $\chi^2 = 2.676$) and the application of anisotropic displacement parameters led to non-physical, disc-like distribution of scattering intensity for the lithium in the octahedron. Positional disorder has been reported at the octahedral position in related compounds and so a refinement was undertaken by moving the lithium cation from the 48*g* position onto an adjacent general position (96*h*) with half of the occupancy. Refinement of this model using isotropic displacement parameters resulted in rapid convergence and a considerable improvement in the fit ($R_{wp} = 1.69$, $\chi^2 = 2.181$). Attempts to refine independent isotropic displacement parameters for the two crystallographically distinct lithium positions destabilised the refinement and so a single isotropic lithium displacement parameter was used. In the related phases $Li_5La_3Nb_2O_{12}$ and $Li_{5+x}Ba_xLa_{3-x}Ta_2O_{12}$, scattering occurred from multiple scattering centres i.e. the refinement required the presence of lithium on both the 48*g* and 96*h* positions. Although a high quality of fit to the $Li_5La_3Sb_2O_{12}$ data had been obtained by using the 96*h* model described above, an additional refinement was undertaken using a mixture of 48*g* and 96*h* lithium positions to model the scattering arising from the octahedron. This failed to provide a substantial improvement to the fit and destabilised the refinement indicating that this model overanalyses the data. Consequently, the final structural model makes use of a tetrahedral position and a single, split octahedral 96*h* site for lithium coordination to give the structural parameters shown in Tables 1 and 2 and the interatomic distances in Table 3 (Figs. 4 and 5).

4. Discussion

4.1. $Li_3Nd_3W_2O_{12}$

The standard garnet stoichiometry of $Li_3Nd_3W_2O_{12}$ permits this compound to adopt the conventional garnet structure with Li^+ fully occupying the tetrahedrally coordinated site in the $[Nd_3W_2O_{12}]^{3-}$ framework. This compound is hence isostructural with the recently reported phases $Li_3Ln_3Te_2O_{12}$ [6]. As W^{6+} and Te^{6+} have ionic radii of 0.60 and 0.56 Å, respectively [19], it would be anticipated that similarities would exist between $Li_3Nd_3W_2O_{12}$ and $Li_3Nd_3Te_2O_{12}$ and inspection of the metal oxide octahedra reveals respective bond lengths of 1.9229(3) and 1.9284(3) Å that support this assumption. The distortion of this octahedron is similar in the two phases as shown by the angles 85.690(12)° and 85.508(13)° for O–W–O and O–Te–O, respectively. Interestingly, the reduction in polarisability on replacing a d^{10} cation (Te^{6+}) with a d^0 cation (W^{6+}) causes significant changes in the bond lengths of lithium and neodymium in these compounds. $Li_3Nd_3W_2O_{12}$ and $Li_3Nd_3Te_2O_{12}$ show Li–O distances of 1.9113(3) and 1.9286(3) Å and mean Nd–O distances of 2.467 and 2.486 Å giving variations of 0.95% and 0.75% in these parameters. This change in Nd–O distance is so large that it approaches the value of the mean separation between samarium and oxide in the isostructural garnet $Li_3Sm_3Te_2O_{12}$ [6]. It is probable that the harder W^{6+} withdraws more electron density from the oxide anion than Te^{6+} and consequently the largely ionic interactions of both Nd^{3+} and Li^+ with oxide require a reduced cation-oxide separation to satisfy their valence requirements. The NdO_8 units form a continuous body-centred lattice that propagates these short Nd–O distances through the structure resulting in a 0.75% difference between the lattice parameters of $Li_3Nd_3W_2O_{12}$ ($a = 12.46869(9)$ Å) and $Li_3Nd_3Te_2O_{12}$ ($a = 12.56253(9)$ Å).

4.2. $Li_5La_3Sb_2O_{12}$

The neutron diffraction data presented here show that the previous space group assignment of $I2_13$ underestimated the symmetry of $Li_5La_3Sb_2O_{12}$ [10]. Describing this compound in $Ia\bar{3}d$ doubles the multiplicity of all cation sites and by increasing the point symmetry of the site occupied by Sb it eliminates the large variation in Sb–O bond lengths previously reported. The application of neutron scattering to this material has also permitted an

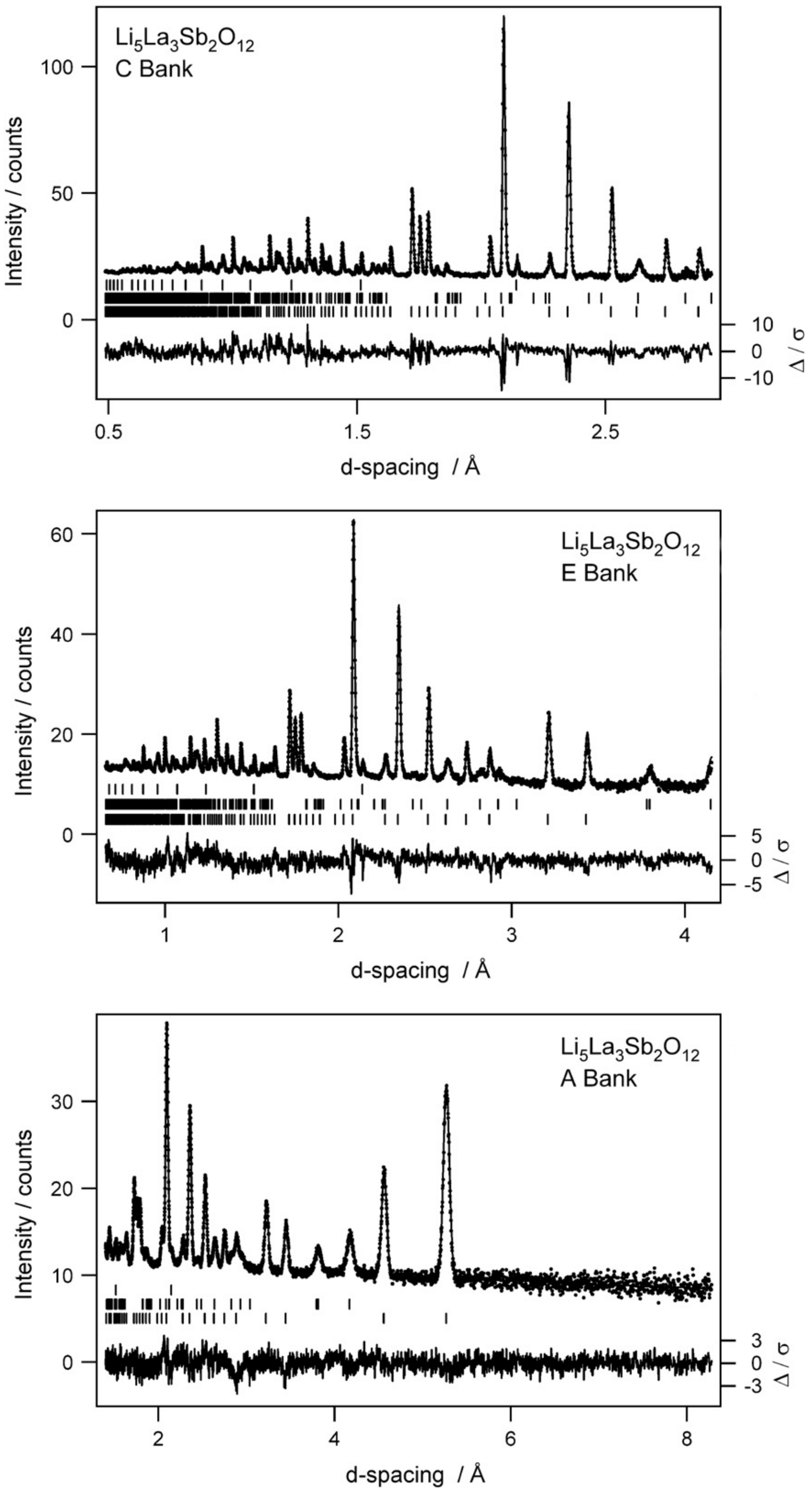

Fig. 4. Observed (dots), calculated (line) neutron diffraction patterns collected from $Li_5La_3Sb_2O_{12}$ using the three banks of detectors of Polaris. The difference is presented as $(I_{obs}–I_{calc})$/[estimated standard deviation of I_{obs}] using the scale on the right axis. Tick marks indicate allowed reflections arising from the garnet (bottom), Li_2CO_3 impurity (middle) and vanadium sample can (top).

accurate determination of the lithium ion distribution for the first time. Whilst the previous report contained Li^+ exclusively in a distorted octahedral coordination environment with an occupancy of $\frac{5}{6}$, this site is actually 53.6(4)% vacant and the lithium is distributed across the octahedron and the tetrahedral sites occupied in conventional garnet

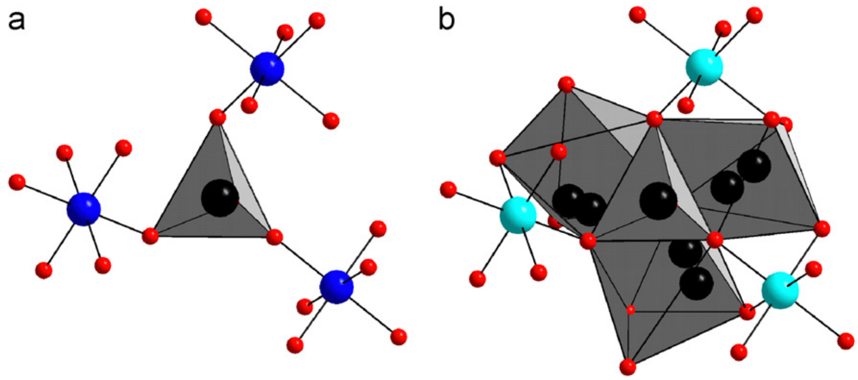

Fig. 5. The lithium cations in (a) $Li_3Nd_3W_2O_{12}$ are found in LiO_4 units (grey tetrahedron) linked through shared apices with tungsten which is octahedrally coordinated by oxide anions. In $Li_5La_3Sb_2O_{12}$ (b) the additional lithium shows positional disorder within distorted LiO_6 units (grey octahedra) that cap each of the four faces of the LiO_4 tetrahedron. Tungsten and antimony are represented by dark and light blue spheres and oxide and lithium are shown by red and black spheres, respectively.

structures, which are 79.3(8)% occupied in $Li_5La_3Sb_2O_{12}$. Thus the lithium distribution in $Li_5La_3Sb_2O_{12}$ is similar to $Li_5La_3Ta_2O_{12}$ and $Li_5La_3Nb_2O_{12}$ which show ca. 82% and 41% occupancies of the oxide tetrahedra and octahedra, respectively. Due to the different sites multiplicities, this results in an equal number of lithium cations occupying each of these two polyhedra [12]. The lithium distribution of $Li_5La_3Sb_2O_{12}$ differs from $Li_5La_3Ta_2O_{12}$ and $Li_5La_3Nb_2O_{12}$ in the complexity of the disorder. In these compounds, the oxide octahedron clearly contains lithium on a central 48*g* position as well as the displaced 96*h* site observed in $Li_5La_3Sb_2O_{12}$. Whilst disorder is notoriously difficult to model accurately, the observation of a smooth evolution in the occupancies of these two sites as a function of composition in $Li_{5+x}Ba_xLa_{3-x}Ta_2O_{12}$ indicates that this multiple lithium position is a robust finding for this system [13]. The inability of the $Li_5La_3Sb_2O_{12}$ data to define two separate lithium displacement parameters for the 24*d* and 96*h* positions provides some indication that the structural model is approaching the sensitivity limits of the neutron diffraction data. We suspect that the limit originates from the use of natural abundance lithium rather than samples enriched with ^7Li although uncertainties in the isotopic distribution of the supplied reagents make this difficult to verify. Regardless of origin, the limitations in the $Li_5La_3Sb_2O_{12}$ data suggest that the refined lithium position is an over-simplification of the true lithium distribution in $Li_5La_3Sb_2O_{12}$. Certainly, the interatomic distances derived from this refinement suggest implausibly short Li–O bonds and it is likely that this lithium position represents an averaged observation that is unrepresentative of local lithium environments.

Despite the slight reduction in the ionic radius of Sb^{5+} (0.60 Å) compared to Ta^{5+} and Nb^{5+} (both 0.64 Å) [19], the Sb–O distance 1.9914(6) Å is only marginally less than the analogous distances in $Li_5La_3Ta_2O_{12}$ and $Li_5La_3Nb_2O_{12}$. Interestingly, the effect of Sb^{5+} is most noticeable in the change in the mean La–O bond lengths which increase from 2.53705 (Ta) and 2.53145 (Nb) to 2.5524 Å (Sb) leading to an increase in the lattice parameter from 12.80654(11) (Ta) and 12.79432(11) (Nb) to 12.8518(3) Å for $Li_5La_3Sb_2O_{12}$. Thus the finding of a reduction in unit cell size on moving from a d^{10} M^{6+} cation to a d^0 M^{6+} cation in the $Li_3Nd_3M_2O_{12}$ system described above is reproduced in $Li_5La_3M_2O_{12}$ for pentavalent cations.

5. Conclusions

Neutron diffraction experiments have shown that the previously undetermined structure of $Li_3Nd_3W_2O_{12}$ is isomorphous with the tellurate analogue and contains lithium exclusively on a filled tetrahedrally coordinated site. The symmetry of $Li_5La_3Sb_2O_{12}$ has been underestimated in the literature and contains a more complex distribution of lithium cations over the same tetrahedral site, which is 79% occupied, and a distorted oxide environment which contains strongly displaced lithium in 44% of octahedra. At this level of description, $Li_5La_3Sb_2O_{12}$ is isostructural with $Li_5La_3Ta_2O_{12}$ and $Li_5La_3Nb_2O_{12}$. The apparently simpler lithium disorder in the antimonate is due to limitations in the neutron diffraction data and no significant difference exists between the lithium distributions in the tantalate, niobate and antimonate garnets. Both $Li_3Nd_3M_2O_{12}$ and $Li_5La_3M_2O_{12}$ show that for d^0 compounds the *Ln*–O distance is reduced leading to a reduction in the unit cell volume compared to the d^{10} analogues. The addition of a tungstate and an antimonate to the family of lithium-containing garnets shows that this set of compounds exhibits a considerable range of cell sizes, stoichiometries and compositions and suggests a number of variables to influence the lithium mobility in this structure.

Acknowledgments

The authors are grateful to the Royal Society for the provision of a University Research Fellowship, to EPSRC and the University of Strathclyde for funding and to Dr. R. Smith for assistance with the neutron diffraction experiments.

Appendix A. Supplementary materials

Supplementary data associated with this article can be found in the online version at doi:10.1016/j.jssc.2007.04.007.

References

[1] S.C. Abrahams, S. Geller, Acta Crystallogr. 11 (1958) 437.

[2] H.M. Kasper, Inorg. Chem. 8 (1968) 1000.

[3] V. Thangadurai, H. Kaack, W.J.F. Weppner, J. Am. Ceram. Soc. 86 (2003) 437.

[4] V. Thangadurai, W. Weppner, Adv. Funct. Mater. 15 (2005) 107.

[5] V. Thangadurai, W. Weppner, J. Solid State Chem. 179 (2006) 974.

[6] M.P. O'Callaghan, D.R. Lynham, G.Z. Chen, E.J. Cussen, Chem. Mater. 18 (2006) 4681.

[7] H. Hyooma, K. Hayashi, Mater. Res. Bull. 23 (1988) 1399.

[8] D. Mazza, Mater. Lett. 7 (1988) 205.

[9] J. Isasi, M.L. Veiga, R. Saez-Puche, A. Jerez, C. Pico, J. Alloys Compds. 177 (1991) 251.

[10] J. Isasi, M.L. Veiga, A. Jerez, C. Pico, J. Less-Common Met. 167 (1991) 381.

[11] V. Thangadurai, W. Weppner, Ionics 12 (2006) 81.

[12] E.J. Cussen, Chem. Commun. (2006) 412.

[13] M.P. O'Callaghan, E.J. Cussen, Chem. Commun., in press.

[14] S. Heinemann, R. Miletich, Am. Mineral. 85 (2000) 993.

[15] V. Thangadurai, S. Adams, W. Weppner, Chem. Mater. 16 (2004) 2998.

[16] M.L. Lopez, M.L. Veiga, J. Rodriguez-Carvajal, Mater. Res. Bull. 27 (1992) 647.

[17] H.M. Rietveld, Acta Crystallogr. 2 (1969) 65.

[18] A.C. Larson, R.B. von Dreele, General Structure Analysis System (GSAS), Los Alamos National Laboratories, 1990.

[19] R.D. Shannon, Acta Crystallogr. A 32 (1976) 751.